Nonlinear Dynamics manuscript No.
(will be inserted by the editor)

Impulsive stabilization of chaos in fractional-order systems

Marius-F. Danca · Michal Fečkan · Guanrong Chen

Received: date / Accepted: date

Abstract This paper considers a class of nonlinear impulsive Caputo differential equations of fractional order, which models chaotic systems. Computer-assisted proof of chaos suppression by stabilizing the unstable system equilibria is provided. A non-existence result of periodic solutions is presented and the commensurate fractional-order Lorenz system is simulated for illustration.

Keywords Impulsive Caputo differential equation of fractional order; Adams-Bashforth-Moulton method; chaos stabilization

1 Introduction

The concept of impulsive control has a long history and its mathematical foundation called impulsive differential equations can be traced back to the beginning of the control theory. Many impulsive control methods were successfully developed under the framework of optimal control and were occasionally called impulse control. Nowadays there is a tendency of integrating impulsive control into hybrid control systems. In mechanical systems, impulsive phenomena had been studied for different scenarios such as mechanical systems with impacts. Impulsive systems can only be studied by the mathematical tool based on impulsive differential equations. The study of impulsive control problems had been restricted to only a few kinds of special problems such as mechanical systems with impacts and the optimal control of spacecraft [1]. In the last two decades, impulsive differential equations had been intensively studied and impulsive differential equations were found in e.g. nanoelectronic devices and chaotic spread-spectrum communication systems as well in electrical engineering applications.

The main reason that only integer-order systems had been considered till recently was the absence of methods to find the solutions of differential equations of fractional order. Today, the more than 300 years old fractional calculus (see e.g. monographies [2,3]), is revised via many numerical methods to approximate fractional-order derivatives and integrals [4,5]. As a consequence, the number of applications of fractional derivative equations (FDEs) is growing continuously [6]. Nowadays, FDEs serve as good models in mechatronics, viscoelasticity, aerodynamics, seismology, biophysics, electrical circuits, biology, blood flow phenomena, fluid flows, chemistry, control theory, etc. Also, since fractional-order systems present infinite memory and hereditary properties, they are ideal models for neural systems [7,8].

Marius-F. Danca · corresponding author
Department of Mathematics and Computer Science,
Avram Iancu University of Cluj-Napoca, 400380 Cluj-Napoca, Romania,
and
Romanian Institute of Science and Technology,
400487 Cluj-Napoca, Romania
E-mail: danca@rist.ro

Michal Fečkan
Department of Mathematical Analysis and Numerical Mathematics, Faculty of Mathematics, Physics and Informatics, Comenius University in Bratislava, Mlynská dolina, 842 48 Bratislava, Slovak Republic,
and
Mathematical Institute, Slovak Academy of Sciences, Štefánikova 49, 814 73 Bratislava, Slovak Republic
E-mail: Michal.Feckan@fmph.uniba.sk

Guanrong Chen
Department of Electronic Engineering,
City University of Hong Kong, Hong Kong, China
E-mail: eegchen@cityu.edu.hk

The most widely known integration methods for FDEs are the frequency-based methods [10], the Adams-Bashfroth-Moulton numerical predictor-corrector scheme [11] (which exhibits the long-term memory property of the underlying system) and methods based on the Grünwald-Letnikov definition of fractional derivatives [6, 12].

Chaos control or stabilization, on the other hand, suppresses completely or reduces significantly chaotic oscillations toward regular movements. Controllers designed for stabilization of chaos in integer-order systems [13] have also been used to stabilize fractional-order systems ([14–17]).

In the last few years, chaos control, including stabilization of unstable equilibria and more generally unstable periodic orbits was the subject of a large number of research works. As a result many methods for chaos suppression, such as the OGY method, state-feedback control method and delayed-feedback control, have been developed [18–23].

In the last decades, impulsive DEs and impulsive FDEs attracted increasing attention from researchers in engineering, biology, physics, and the like. Based on the Dirac delta function, Impulsive Fractional-order Differential Equations (IFDE) can model processes with abrupt changes, which cannot be described with classical differential problems (see [24–29] and references therein). For comparison, impulse integer-order differential equations and related issues, i.e., stability, control etc. can be found in the monograph [30].

In this paper, impulsive control is used to stabilize chaotic behavior of fractional-order systems. For a right choice of impulses and time moments, the controlled trajectories could reach a stable equilibrium. This equilibrium is situated closely to one of the system unstable equilibria of the non-controlled system. The approach applies to a large class of nonlinear fractional-order systems such as Rössler, Chua, Lorenz, Chen, Rabinovich-Fabrikant, and Lotka-Volterra systems. The advantage of the proposed impulsive chaos stabilization method consists in the fact that it can be applied to one or several state variables and at different time moments. Also, it is analytically proved that exact periodic solutions of impulsive FDEs can exist.

The rest of the paper is organized as follows: Section II presents some preliminary results. In Section III, impulsive chaos control with its numerical implementation are described and the case of commensurate fractional-order Lorenz system is illustrated. A recent problem of non-existence of exact periodic orbits of fractional-order systems for the case of impulsed fractional-order Lorenz system is presented and analytically proved. The paper is ended by a short conclusion.

2 Notions and preliminaries results

2.1 Impulsive fractional-order equations

Definition 1 Let $q \in (0,\infty)\setminus\mathbb{N}$, $n=[q]+1$ and some function $f \in C^n([a,b],\mathbb{R})$. The fractional-order Caputo derivative of order q of f is

$$ {}^{C}D_{a+}f(t) = \frac{1}{\Gamma(n-q)}\int_a^t (t-s)^{n-q-1} f^{(n)}(s)ds,$$

where Γ is a Gamma function which, defined via the Euler integral, is $\Gamma(x)=\int_0^\infty t^{x-1}e^{-t}dt$ $(x>0)$.

Notation 2 *The fractional-order Caputo derivative of order q with starting point 0 will be denoted by D_*^q hereafter.*

Consider the initial value problem for the following IFDEs of the Caputo type:

$$\begin{aligned} &D_*^q x(t) = f(t,x(t)), \quad \text{for } t\in I=[0,T]\setminus\{t_k\}_{k=1}^N,\\ &x(t_k^+) = x(t_k^-) + \Delta_k\big|_{t=t_k},\ t_k\in I,\ k=1,2,...,N,\\ &x(0)=x_0, \end{aligned} \tag{1}$$

where $f: I\times\mathbb{R}^n\to\mathbb{R}^n$, $\Delta_k:\mathbb{R}\to\mathbb{R}$, $x_0\in\mathbb{R}^n$, $0=t_0<t_1<\cdots<t_N<t_{N+1}=T$, and $x(t_k^+)=\lim_{\delta\downarrow 0}x(t_k+\delta)$ and $x(t_k^-)=\lim_{\delta\uparrow 0}x(t_k-\delta)$ represent the right and left limits of $x(t)$ at $t=t_k$.

Because the use of Caputo's derivative, in (1) the initial conditions can be considered as that for classical ordinary differential equations [31].

The existence of solutions of the Impulsive Fractional-order Problem (IFP) (1) is given by the following theorem.

Theorem 1 *[25] Assume that:*

(H1) *$f: I\times\mathbb{R}^n\to\mathbb{R}^n$ is uniformly continuous and globally Lipschitz in x for $t\in[0,T]$.*

(H2) *There exists a constant $M>0$ such that $|f(t,u)|\le M$ for each $t\in I$ and each $u\in\mathbb{R}$.*

(H3) *The functions $\Delta_k:\mathbb{R}\to\mathbb{R}$ are continuous and there exists a constant $M^*>0$ such that $|\Delta_k(u)|\le M^*$ for all $u\in\mathbb{R}$, $k=1,2,...,N$.*

Then, the IVP (1) admits a unique solution on I.

For more details, see also [6,24].

2.2 Stability of fixed points

Consider the nonlinear system

$$D_*^q x = f(x),$$

let X^* be an equilibrium, J_{X^*} be the Jacobian matrix $J = \partial f/\partial x$ evaluated at X^*, and Λ be the spectrum of all eigenvalues of J.

Theorem 2 *[32,33] Equilibrium X^* is*
-asymptotically stable iff $|\arg(\Lambda)| > q\pi/2$;
-stable iff either is asymptotically stable, or its critical eigenvalues satisfying $|\arg(\Lambda)| = q\pi/2$ have geometric multiplicity one.

The function $\arg(\lambda) \in (-\pi, pi]$, $\lambda \in \mathbb{C}$, is the principal branch of the set-valued function $Arg(\lambda)$, which can be determined with e.g. the Matlab *atan*2 function.
If there exists some eigenvalue λ for which

$$|\arg(eig(\lambda))| < q\pi/2,$$

then X^* is unstable. The inequality represents a necessary condition for a chaotic behavior [33].

2.3 Generalized Hamiltonian energy

The Helmholtz theorem (or fundamental theorem of vector calculus) [34] allows to decompose a smooth vector field, which defines most physical systems such the Lorenz, Chen, Rössler systems by a sum of two vectors: an irrotational part (curl-free) and a solenoidal part (divergence-free): $f = f_c + f_d$. Thus, f_d carries the divergence of f (i.e. $curl(f_d) = 0$), while f_c takes account of the whole rotor of f (i.e. $div(f_c) = 0$). The energy storage corresponds to f_c, while the energy consumption corresponds to f_d.

As described in [35], using Helmoltz's theorem, it is possible to find a specific function with the characteristic of energy (generalized Hamiltonian), H, which describes the absorbtion or dissipation of energy in a chaotic system. Therefore, it is possible to describe the dynamics of the IFDE (1) in terms of the Hamiltonian energy required by the system to stabilize chaos therein.

The (non-unique) Hamiltonian function can be found by solving the following PDE [35,36]:

$$\nabla H^T f_c(x) = 0, \tag{2}$$

which leads to solving the system

$$\frac{dx_1}{f_c^1(x)} = \frac{dx_2}{f_c^2(x)} = \cdots = \frac{dx_n}{f_c^n(x)}. \tag{3}$$

where $f_c = (f_c^1, f_c^2, ..., f_c^n)^T$.

The derivative of H, which indicates the rate of change of the energy H, is obtained as

$$\dot{H} = \frac{dH}{dt} = \nabla H^T f_d(x). \tag{4}$$

3 Chaos suppression in impulsive fractional-order systems

Consider the autonomous IFDE (1), along with constant impulses $(\Delta_{k,1}, \Delta_{k,2}, \cdots, \Delta_{k,p})^T$ periodically applied to $p \leq n$ variables x_i at different moments of time $t_{k,i}$, $i = 1, 2, \cdots, p \leq n$, $k = 1, 2, ..., N$; more precisely,

$$\begin{aligned} &D_*^q x(t) = f(x), \quad \text{for } t \in I = [0,T] \setminus \{t_{k,i}\}_{k=1}^N,\ i = 1, 2, ..., p \leq n, \\ &x_i(t_{k,i}^+) = x_i(t_{k,i}^-) + \Delta_{k,i}\big|_{t=t_{k,i}},\ t_{k,i} \in I,\ k = 1, 2, ..., N, \\ &x(0) = x_0, \end{aligned} \tag{5}$$

where $f : \mathbb{R}^n \to \mathbb{R}^n$, $\Delta_{k,i} : \mathbb{R} \to \mathbb{R}$, $i = 1, 2, ..., p \leq n$, $k = 1, 2, ..., N$, $x_0 \in \mathbb{R}$.

Generally, IFDE (1) refers to simultaneously applying impulses operators $\Delta_{k,i}$ to some variables at the time moments t_k, $k = 1, 2, ..., N$. Here, consider a more general case when impulses $\Delta_{k,i}$ can be applied at different time moments $t_{k,i}$, $k = 1, 2, ..., N$, for each variable x_i,$i = 1, 2, ..., p \leq n$.

To implement this kind of impulses, one may associate to each variable x_i its own strictly increasing sequence of time moments $t_{k,i} = k \times m_i \times h$, $k = 1, 2, ..., N$, with $N = T/h$, m_i some positive integer and $h > 0$ the step-size of the utilized numerical method to integrate the IVP (5). Thus, for every variable x_i, I will be partitioned as follows: $0 = t_{0i} = 0m_ih < t_{1,i} = 1m_ih < t_{2,i} = 2m_ih < t_{3,i} = 3m_ih < \cdots < t_{N,i} = Nm_ih < t_{N+1,i} = (N + 1)m_ih = T$, $i \in \{1, 2, ..., p\}$. In this way, variables x_i will be impulsioned at different (possible identical) time moments: $t_{k,i} \neq t_{k,j}$, for $i \neq j$ and $i, j \in \{1, 2, ..., p\}$, $1 \leq k \leq N$.

Notation 3 *For simplicity, $t_{k,i}$ will be denoted by t_i, and $\Delta_{k,i}$ by Δ_i, $i \in \{1, ..., p\}$, while $\Delta_i = 0$ correspond to non-impulsed variables.*

For example, for $n = 3$, by $(\Delta_1, 0, \Delta_3)^T$ and $(t_1, t_3) = (kh, 2kh)$ one understands that only x_1 and x_3 are impulsed at the time moments kh and $2kh$, $m_1 = 1$ and $m_3 = 2$, $k = 1, 2, ..., N$, with Δ_1 and Δ_3, respectively.

The existence and uniqueness of solutions to (5) is ensured by Theorem 1.

If the considered nonlinear dynamical system has unstable equilibria and evolves chaotically, it can be shown numerically that there are several possible choices of impulses, considered as control applied to x_i at right time moments t_{ki}, such that chaos can be controlled for stabilizing the unstable equilibria. As a result, after some transients, the trajectory reaches some stable equilibrium.

The stability of the controlled equilibria is checked with Theorem 2, and verified with the monotony of a generalized energy H, time series and phase plots.

3.1 Application

In this paper, a *constant solution* refers to a numerical solution determined within 6 decimals because of the numerical accuracy and digital resolution, namely the used software (Matlab) and the integration ABM method (see Fig. 1, where the control is turned on at $t = t_1$ and turned out at $t = t_2$). As can be seen in the zoomed rectangle in Fig. 1, 6 decimals are enough to ensure a reasonable error of $1E-6$ for numerical studies. Therefore, with the integration step-size $h = 0.004$ chosen in this paper, the obtained trajectories can be considered constant within the time interval $I = [0, 100]$. Accordingly, $N = T/h = 100/0.004 = 25,000$.

The stability of equilibria is verified with Theorem 2. After applying the impulsive chaos control, and after transients are removed, trajectories become constant and reach a point close to one unstable equilibrium.

the stability of the reached points is verified numerically

In order to preserve the Time-history dependence of solutions, required by Caputo's fractional-derivative, the multi-step predictor-corrector Adams-Bashforth-Moulton method for FDEs [11] is utilized here is adopted), which at every solution point takes account on the entire previous points.

To implement the impulses, at every kth step, $k = 1, 2, ..., N$, after the ith variable $x_{k,i}$ is calculated, the following tests are added: $if\ k\ mod\ m_i = 0$, for $i = 1, ..., p$, then the variable $x_{k,i}$ will be modified as $x_{k,i} = x_{k-1,i} + \Delta_i$.

Next, consider the fractional Lorenz system with the commensurate fractional-order $q = 0.995$[1], given by

$$\begin{aligned} D_*^{0.995}x_1 &= a(x_2 - x_1), \\ D_*^{0.995}x_2 &= x_1(b - x_3) - x_2, \\ D_*^{0.995}x_3 &= x_1x_2 - cx_3, \end{aligned} \tag{6}$$

where a, b, c are the standard Lorenz parameters: $a = 10$, $c = 8/3$ and b is chosen in some chaotic windows (see the bifurcation diagram in Fig. 2). With $b = 28$, the system evolves chaotically (Fig. 3).

For all simulations, x_0 is chosen $x_0 = (0.1, 0.1, 0.1)$.

The equilibria of the unperturbed system are

$$X_{1,2}^* = \pm\Big(\sqrt{c(b-1)}, \sqrt{c(b-1)}, c-1\Big)^T = \pm(8.46, 8.46, 27)^T.$$

The spectrum of eigenvalues of $X_1^* = (8.46, 8.46, 27)^T$ is $\Lambda = \{\lambda_1 = -13.846, \lambda_2 = 0.090 - 10.166i, \lambda_3 = 0.090 + 10.166i\}$ with arguments $\{\pi, -1.5620, 1.5620\}$. Since there exist the eigenvalues $\lambda_{2,3}$, for which $|arg(\lambda_{2,3})| - 0.995\pi/2 = 1.5620 - 1.5787 < 0$, by Theorem 2, X_1^* is unstable. The same reasonings apply to X_2^*. Therefore, for $b = 28$ both equlibria $X_{1,2}^*$ are unstable and the system behaves chaotically.

[1] The fractional-order has been chosen close to 1, such that chaos is as strong as possible (note that the minimum order for the fractional-order Lorenz system to be chaotic is $q = 0.99$ [37]).

3.2 Case 1: identical impulses at the same time moments

Let $(\Delta_1, \Delta_2, \Delta_3)^T = (\Delta, \Delta, \Delta)^T$ be applied to all variables at the same time moments $(t_1, t_2, t_3) = (kh, kh, kh)$, $k = 1, 2, ..., N$. For example, with identical impulses $(\Delta_1, \Delta_2, \Delta_3)^T = (0.04, 0.04, 0.04)^T$ being applied at the same time moments: $(t_1, t_2, t_3) = (kh, kh, kh)$, $k = 1, 2, ..., N$, to all variables, which means that every integration step is h, all variables are under the effect of the same impulse 0.04. One obtains the results presented in Fig. 4 (a) (phase plot) and Figs. 4 (b)-(d) (time series). These indicate that, after some short transients, the trajectory reaches the point $Y_1^* = (y_1^*, y_2^*, y_3^*)^T = (8.58, 7.61, 28.22)^T$.

By applying the stability criteria to the point Y_1^*, one obtains $\Lambda = \{-13.152, -0.257 - 10.469i, -0.2572 + 10.4691i\}$ with arguments $\{\pi, \pm 1.5954\}$ and $|\arg(\Lambda)| > q\pi/2$. Therefore, the point reached by the trajectory under impulsive control, Y_1^*, is stable. The Euclidean distance in the phase space between X_1^* and Y_1^*, $d(X_1^*, Y_1^*) = |X_1^* - Y_1^*| < 1.5$. This relatively large distance is due to the impulsive effect on the system variables, which had slightly changed the system dynamics. However, it is relatively small as compared to the size of the chaotic attractor in the phase space which, for $b = 28$, can be embedded in the sphere (see Fig.5)[2]

$$\mathcal{S} = \{(x_1, x_2, x_3) \in \mathbb{R}^3 : x_1^2 + x_2^2 + (x_3 - a - b)^2 \leq R^2$$

with $R = (a + b)c/\sqrt{4(c - 1)} = 39.25$ and center $(0, 0, a + b)$ [38]. Thus, $d(X_1^*, Y_1^*)/2R \approx 0.01$, and the impulsive chaos control can be considered as stabilizing the unstable equilibrium X_1^*.

The best way to choose the impulses $(\Delta, \Delta, \Delta)^T$ in the case of identical impulses is to build a bifurcation diagram with bifurcation parameter Δ (see Fig. 6, where $\Delta \in [-0.5, 0.5]$).

3.3 Case 2: All variables with different impulses at different time moments

For $(\Delta_1, \Delta_2, \Delta_3)^T = (0.01, -0.05, 0.02)^T$ and $(t_1, t_2, t_3) = (3kh, kh, 2kh)$, the controlled trajectory reaches the stable point $Y_2^* = (-8.53, -8.58, 28.40)^T$ (see Fig.7) situated at distance $d(X_2^*, Y_2^*) < 1.5$.

3.4 Case 3: Some variables with different impulses at different time moments

Consider the case $(\Delta_1, \Delta_2, \Delta_3)^T = (0, -0.02, 0.02)^T$ applied at moments $(t_2, t_3) = (kh, 2kh)$, to variables x_2 and x_3. One obtains $Y_2^* = (-8.29, -8.29, 27.58)^T$ (see Fig. 8). In this case, Y_2^* is closer to X_2^*: $d(X_1^*, Y_1^*) = |X_1^* - Y_2^*| < 0.7$ and, again, Y^* verifies the stable criterion.

3.5 Case 4: A single variable

Use $(\Delta_1, \Delta_2, \Delta_3)^T = (0, 0, 0.05)^T$, $t_3 = kh$. Then, the impulsed system reaches the stable point $Y_2^* = (-7.74, -7.74, 26.97)$ (see Fig. 9). Now, $d(X_2^*, Y_2^*) < 1.1$.

3.6 Energy approach

For the Lorenz system, the Helmoltz decomposition yields [35,36]

$$f_c(x_1, x_2, x_3) = \begin{pmatrix} ax_2 \\ bx_1 - x_1x_3 \\ x_1x_2 \end{pmatrix}, \quad f_d(x_1, x_2, x_3) = \begin{pmatrix} -ax_1 \\ -x_2 \\ -cx_3 \end{pmatrix}.$$

In solving practical problems, f_d can be determined by having all the terms in f, which contribute to divergence, and the rest of the terms are represented by f_c.

To calculate H, one needs to solve the linear partial differential equation (see (2)):

$$\nabla H^T f_c(x_1, x_2, x_3) = 0,$$

which leads to the following system of equations (see (3))

$$\frac{dx_1}{ax_2} = \frac{dx_2}{bx_1 - x_1x_3} = \frac{dx_3}{x_1x_2},$$

whose one solution is

[2] Once the trajectory enters the sphere, it remains inside.

Table 1 Average energy $\overline{H}$, average of derivative energy $\overline{\dot{H}}$ for the impulsive system (1), and average energy of non-impulsive system, $\overline{H_0}$.

b	Δ	t_k	$\overline{H}$	$\overline{\dot{H}}$	$\overline{H_0}$	Figure
28	$(0.04, 0.04, 0.04)^T$	(kh, kh, kh)	324	-96	270	Fig. 10 (a)
28	$(-0.04, -0.04, -0.04)^T$	(kh, kh, kh)	300	496	270	Fig 10 (b)

$$H(x_1, x_2, x_3) = \frac{1}{2}\Big(-\frac{b}{a}x_1^2 + x_2^2 + x_3^2\Big). \tag{7}$$

Unlike the H given by (7), the Lyapunov function commonly used for analyzing the Lorenz system is a quadratic positive definite function $V(x_1, x_2, x_3) = bx_1^2 + ax_2^2 + a(x_3 - 2b)^2$, which might fail to unveil some system dynamical characteristics.

The derivative of H, which gives the rate of energy changes, can be obtained by imposing the condition that the change of the energy along some trajectory is exclusively due to the term f_d (see (4)), yelding

$$\dot{H}(x_1, x_2, x_3) = \nabla H^T f_d(x_1, x_2, x_3) = bx_1^2 - x_2^2 - cx_3^2. \tag{8}$$

Next, the average of H, $\overline{H}$, and the average of $\dot{H}$, $\overline{\dot{H}}$, are calculated after their first transients have been removed. The energy is considered in any unit, so $\dot{H}$ can be considered as describing the energy changes per unit time [35].

Two representative cases have been considered for a clear understanding of what happens with the energy while the impulses are applied.

In Fig. 10 (a), $\overline{H}$ and $\overline{\dot{H}}$ are plotted for the impulses $(\Delta_1, \Delta_2, \Delta_3)^T = (0.04, 0.04, 0.04)^T$ applied at moments $(t_1, t_2, t_3) = (kh, kh, kh)$. In Fig. 10 (b), the impulses $(\Delta_1, \Delta_2, \Delta_3)^T = (-0.04, -0.04, -0.04)^T$ are applied at time moments $(t_1, t_2, t_3) = (kh, kh, kh)$. The results are summarized in Table 1.

As expected for the obtained equilibria $Y^*_{1,2}$, after some transients the energy H dissipated or absorbed by the system remains constant, just like the variation of $\dot{H}$. The variation of the energy at local extrema of $\dot{H}$ is 0, while the maximum (minimum) variation of the energy appear before (after) the energy attaints a local maximum (se the zoomed detail in Fig. 10 (c)). As expected, this normally happens at extrema of the trajectories, where the vanished derivative of H, regarded as a 0 kinetic-like energy, implies a maximum potential-like energy in these extrema of trajectories, capable of driving the trajectory further to the next extremum.

Note that for equilibria $Y^*_{1,2}$ the average energy of the impulsive system is higher than the non-impulsive system, denoted by H_0 (see Table 1, lines 1,2). Also, in these cases, positive impulses determine a negative variation of energy (Table 1, line 1), which means that the system dissipates energy to maintain the trajectory at the stable equilibrium Y^*. Negative impulses (Table 1, line 2) determine a positive variation of energy to maintain the trajectory at the obtained stable equilibrium Y^*. This means that the system needs energy in both cases.

No concluding results have been obtained if the Δ components have opposite signs.

4 Discussion

In the above, it was shown numerically that the chaotic behaviors in fractional-order systems can be stabilized by stabilizing their unstable equilibria with periodic constant impulses applied to all or some variables, and the obtained trajectories becoming constant after transients being removed.

However, if for Lorenz system one considers $b = 120$, for which the system still presents a chaotic behavior (see Fig. 2), with appropriate constant impulses $(\Delta, \Delta, \Delta)^T$ chosen from the bifurcation diagram in Fig. 12 with Δ bifurcation parameter, the chaotic behavior can also be transformed to possible "stable cycles". For example, for $(\Delta_1, \Delta_2, \Delta_3)^T = (0.0665, 0.0665, 0.0665)^T$ applied at time moments $(t_1, t_2, t_3) = (kh, kh, kh)$, $k = 1, 2, ..., N$, one obtains the trajectory shown in Fig. 11 (a). Figs. 11 (b)-(d) present the time series of the three variables $x_{1,2,3}$.

As Figure 6 shows, in the case of equal impulses Δ, for $b = 28$ the chaos can be stabilized, theoretically even for no matter how large values of impulse values Δ. However, positive or negative large values could lead to results without physical meanings. Also, as expected and as Figure 6 reveals, too small values of Δ (the small interval around origin) cannot stabilize the chaos. For the case $b = 120$ (see Figure 12), the windows for Δ where chaos can be stabilized are much more narrow.

The energy approach (Figs. 11 (e)-(f)) indicates a possible periodic behavior. However, this result is in contradiction with the following theorem.

Theorem 3 *[9, 39] The autonomous fractional-order differential equation*

$$D_*^q x(t) = f(x(t)),$$

with f being some nonlinear function, cannot have any non-constant exact smooth periodic solution.

A similar result exists for non-autonomous fractional-order systems (see e.g. [9]).

Therefore, even numerical simulations sometimes suggest that in fractional-order systems there exist "stable cycles", they are only approximations of some non-exactly periodic oscillations, which always contain non-periodic transient terms (see e.g. [39]).

It is well known nowadays that, probably due to the time-history phenomenon of solutions of FDEs [39], autonomous fractional-order systems modeled by Caputo, Riemann-Liouville or Grünwald-Letnikov derivatives, cannot evolve along exact non-constant periodic trajectories for any finite time, except the cases when the lower terminal of the fractional derivative approaches infinity [40]. Thus, if the difference between the lower limit and the upper limit in the concerned derivative are chosen large enough, due to the memory dependence of the derivative, the obtained orbit could be periodic. In other words, while finite-time exact periodic solutions cannot be found in Caputo fractional-order dynamical systems, long-time periodic solutions might be possible [40–42].

For the case of IFDEs, to the best of our knowledge, there exist no results on the existence of exact non-constant periodic solutions[3].

However, the following is a result regarding the non-existence of periodic solutions to the IFDE (1).

In (1) let $T = (N+1)h$. The objective now is to find a periodic solution of (1) satisfying $x(0) = x(T)$. Following [43], by a solution of (1) means a function $x(t)$ that is continuous in $x_0 \in \mathbb{R}^n$, $t \in [0, T] \setminus \{kh \mid k = 1, \cdots, N\}$, and left continuous in t at the impulsive points kh, and satisfying

$$x(t) = x_0 + \sum_{i=1}^{k} \Delta_i + \frac{1}{\Gamma(q)} \int_0^t (t-s)^{q-1} f(s, x(s)) ds, \quad t \in (t_k, t_{k+1}]. \tag{9}$$

It is well known that under the above assumptions, (9) has a unique solution $x(x_0, t)$ on $[0, T]$.

Now the following theorem can be established.

Theorem 4 *Suppose that assumptions **(H1),(H2)** are satisfied. If*

$$\frac{\left\| \sum_{k=1}^{N} \Delta_k \right\|}{(N+1)^q} > \frac{Mh^q}{\Gamma(q+1)}, \tag{10}$$

then (1) *has no (periodic) solutions satisfying $x(0) = x(T)$.*

Proof One needs to solve

$$x(0) = x(T) = x_0 + \sum_{i=1}^{N} \Delta_i + \frac{1}{\Gamma(q)} \int_0^T (T-s)^{q-1} f(s, x(s)) ds,$$

which is equivalent to

$$-\sum_{k=1}^{N} \Delta_k = \frac{1}{\Gamma(q)} \int_0^{(N+1)h} ((N+1)h - s)^{q-1} f(s, x(x_0, s)) ds. \tag{11}$$

This gives

$$\begin{aligned} \left\| \sum_{k=1}^{N} \Delta_k \right\| &\le \frac{1}{\Gamma(q)} \int_0^{(N+1)h} ((N+1)h - s)^{q-1} |f(s, x(x_0, s))| ds \\ &\le \frac{M(N+1)^q h^q}{\Gamma(q+1)}, \end{aligned}$$

contradicting (10). The proof is thus completed.

□

[3] Some related works will be published elsewhere later.

Remark 1 Theorem 4 just states nonexistence of solutions satisfying $x(0) = x(T)$. This is the so-called periodic boundary value condition on $[0, T]$. On the other hand, contrary to FDEs, which does not have periodic exact non-constant solutions, for the IFDE (1), if condition (4.2) is not satisfied, then the IFDE may have a solution on $[0, T]$ satisfying $x(0) = x(T)$, under some additional conditions.

As example, let consider the case for $b = 120$ presented in Fig. 11. As can be observed, the trajectory can be considered as embedded within the domain

$$\mathcal{C} = \{(x_1, x_2, x_3) \in \mathbb{R}^3 : -50 \leq x_1 \leq 50,\ -100 \leq x_2 \leq 100,\ 50 \leq x_3 \leq 200\}.$$

Therefore,

$$M = \max_{x \in \mathcal{C}} \|f(x)\| = \max_{x \in \mathcal{C}} \max\{|a(x_2 - x_1)|, |x_1(b - x_3) - x_2|, |x_1 x_2 - c x_3|\} \doteq 533.333.$$

For $h = 0.004$, $q = 0.995$, by applying $(\Delta_1, \Delta_2, \Delta_3 = (0.0665, 0.0665, 0.0665)$ at time moments kh, $k = 1, 2, ..., N$ and $N = 25000$ one obtains

$$\frac{\left\|\sum_{k=1}^{N} \Delta_k\right\|}{(N+1)^q} = 0.070 < 2.199 = \frac{Mh^q}{\Gamma(q+1)}.$$

Therefore, Theorem 4 rules out that for this example it is possible that the obtained impulsed trajectory drawn in Fig. 11 could be a real stable cycle.

While the bifurcation diagram in Fig. 12 indicates that the chance to choose randomly values for $(\Delta, \Delta, \Delta)^T$ to stabilize chaos for $b = 120$ is rather small, the situation is totally different in the case of $b = 28$, where the bifurcation diagram shown in Fig. 6 indicates that random impulse values, applied following some time moments partition, have more chances to stabilize the chaotic behavior of the system.

Conclusion

In this paper it has been shown numerically that for appropriate impulses and time moments, chaos in impulsive fractional-order differential equations can be stabilized near their unstable equilibria. The unstable equilibria are approximated by stable constant trajectories. The stability of the obtained equilibria is verified numerically. The advantages of the proposed impulsive control, which can be applied to non-commensurate order systems, is that it can act only on some of the state variables and also at different time moments. The disadvantage is the fact that, as all impulsive control techniques, the his applicability is mostly theoretical. In a practical system, measurement noise always exists. Therefore, considering the measurement noise in the numerical results, the proposed impulsive control could reveal his possible application in real systems. This topic will be investigated in future research. The utilized numerical method to integrate the initial value problems is the Adams-Bashforth-Moulton algorithm for fractional-order differential equations. A theorem related to the non-existence of periodic solutions to impulsive fractional-order differential equations has also been presented and proved, which provides some necessary conditions for the periodicity of solutions to IFDE. Thus, compared with FDEs, where exact non-constant periodic solutions cannot exist, the new finding is that for IFDEs these kind of solutions are indeed possible. The results have been verified for the fractional-order Lorenz system, but the control algorithm applies to a large class of systems modeling Chen's system, Lotka-Volterra system, Rössler system, Chua system and so on.

Acknowledgements

The authors thank to Professor Julien Clinton Sprott for interesting discussions related to the energy approach.

M.-F. Danca is supported by Tehnic B SRL. M. Fečkan is supported in part by the Slovak Research and Development Agency under the contract No. APVV-14-0378 and by the Slovak Grant Agency VEGA No. 2/0153/16 and No. 1/0078/17. G. Chen is supported by the Hong Kong Research Grants Council under the GRF Grant CityU 11234916.

References

1. Yang, T.: Impulsive Control Theory. Springer; 2001.
2. Oldham, K., Spainer, J.: Fractional calculus. Academic press; 1974.
3. Podlubny, I.: Fractional Differential Equations. Academic Press; 1989.
4. Baleanu, D., Diethelm, K., Scalas, E., Trujillo, JJ.: Fractional Calculus Models and Numerical Methods, Series on Complexity, Nonlinearity and Chaos: 2012. Volume 3, World Scientific.
5. Sabatier, J., Ionescu, C., Tar, J.K., Teneiro, M.J.A. guest editors. New challenges in fractional systems. 2013. ¡http:// www.hindawi.com/journals/mpe/si/206031.
6. Riccardo, C., Trujillo, J.J., Machado, J.A.T.: Theory and Applications of Fractional Order Systems. Math. Probl. Eng. **2016**, 2016 http://dx.doi.org/10.1155/2016/7903424
7. Arena, P., Caponetto, R., Fortuna, L., Porto, D.: Bifurcation and Chaos in Noninteger Order Cellular Neural Networks. Int. J. Bifurcat. Chaos **8**, 1527-1539 (1998). http://dx.doi.org/10.1142/S0218127498001170
8. Boroomand, A., Menhaj, M.: Fractional-order Hopfield neural networks. In: Lect. Notes. Comp. **5506**, 883-890 (2009)
9. Kaslik, E., Sivasundaram, S.: Non-existence of periodic solutions in fractional-order dynamical systems and a remarkable difference between integer and fractional-order derivatives of periodic functions. Nonlinear Anal.-Real. **13**, 1489-1497 (2012). http://dx.doi.org/10.1016/j.nonrwa.2011.11.013
10. Charef, A., Sun, H.H., Tsao, Y.Y., Onaral, B.: Fractal system as represented by singularity function. IEEE Xplore: IEEE T. Automat. Contr. **37**, 1465 - 1470 (1992). DOI: 10.1109/9.159595
11. Diethelm, K., Ford, N.J., Freed, A.D.: A Predictor-Corrector Approach for the Numerical Solution of Fractional Differential Equations. Nonlinear Dyn. **29**, 3-22 (2002). doi:10.1023/A:1016592219341
12. Scherer, R., Kalla, S.L., Tang, Y., Huang, J.: The Grünwald-Letnikov method for fractional differential equations. Comput. Math. Appl. **62**, 902-917 (2011). http://dx.doi.org/10.1016/j.camwa.2011.03.054
13. Chen, G., Yu, X.: Chaos Control: Theory and Applications. Springer-Verlag; 2003.
14. Oustaloup, A., Sabatier, J., Lanusse, P.: From fractal robustness to the CRONE control. Fractional Calculus & Applied Analysis **2**, 1-30 (1999)
15. Wang, X.-Y., He, Y.-J., Wang, M.-J.: Chaos control of a fractional order modified coupled dynamos system. Nonlinear Anal.-Theor. **71**, 6126-6134 (2009). http://dx.doi.org/10.1016/j.na.2009.06.065
16. Ahmad, W.M., Harba, A.M.: On nonlinear control design for autonomous chaotic systems of integer and fractional orders. Chaos Soliton Fract. **18**, 693-701 (2003). http://dx.doi.org/10.1016/S0960-0779(02)00644-6
17. Boulkroune, A., Chekireb, H., Tadjine, M., Bouatmane, S.: Observer-based adaptive feedback controller of a class of chaotic systems. Int. J. Bifurcat. Chaos **16**, 3411-3419 (2006)
18. Yin, C., Chen, Y.Q., Zhong, S.: Fractional-order sliding mode based extremum seeking control of a class of nonlinear systems. Automatica **50**, 3173-3181 (2014)
19. Yin, C., Cheng, Y., Chen, Y.Q., Stark, B., Zhong, S.: Adaptive fractional-order switching-type control method design for 3D fractional-order nonlinear systems. Nonlinear Dynam. **82**, 39-52 (2015)
20. Chen, G., Dong, X.: From Chaos to Order-Methodologies Perspectives and Applications. World Scientific; 1998.
21. Ott, E., Grebogi, C., Yorke, J.A.: Controlling chaos. Phys. Rev. Lett. **64**, 1196-1199 (1990)
22. Richter, H., Reinschke, K.J.: Local control of chaotic systems-a Lyapunov approach. Int. J. Bifurcat. Chaos **8**, 1565-1573 (1998). http://dx.doi.org/10.1142/S0218127498001212
23. Pyragas, K.: Continuous control of chaos by self-controlling feedback. Phys. Lett. A 170, 421-428 (1992). http://dx.doi.org/10.1016/0375-9601(92)90745-8
24. Agarwal, R.P., Benchohra, M., Slimani, B.A.: Existence results for differential equations with fractional order and impulses. Memoirs on Differential Equations and Mathematical physics **44** 1-21 (2008)
25. Benchohra, M., Slimani, B.A.: Existence and Uniqueness of solutions to impulsive fractional differential equations. Electronic Journal of Differential Equations **2009**, 1-11 (2009)
26. Benchohra, M., Seba, D.: Impulsive fractional differential equations in Banach spaces. Electronic Journal of Qualitative Theory of Differential Equations **2009**, 1-14 (2009)
27. Guan, Z.-H., Chen, G., Ueta, T.: On Impulsive Control of a Periodically Forced Chaotic Pendulum System. IEEE T. Automat. Contr. **45**, 1724 - 1727 (2000). DOI: 10.1109/9.880633
28. Xujun Yang, Chuandong Li, Tingwen Huang, Qiankun Song. MittagLeffler stability analysis of nonlinear fractional-order systems with impulses. Appl. Mth. Comput. **293**, 416422 (2017)
29. Xujun Yang, Chuandong Li, Qiankun Song, Tingwen Huang, Xiaofeng Chen: Mittag-Leffler stability analysis on variable-time impulsive fractional-order neural networks. Neurocomputing **207**, 276286 (2016)
30. Samoilenko, A.M., Perestyuk, N.A.: Impulsive Differential Equations. Series on Nonlinear Science. World Scientific; 1995.
31. Heymans, N., Podlubny, I.: Physical interpretation of initial conditions for fractional differential equations with Riemann-Liouville fractional derivatives. Acta Rheologica **45**, 765-771 (2006). Doi: 10.1007/s00397-005-0043-5
32. Matignon, D.: Stability results of fractional differential equations with applications to control processing. In: IEEE-SMC proceedings of the Computational engineering in systems and application multiconference. IMACS; 1996. Vol. 2, p. 963-968.
33. Tavazoei, M.S., Haeri, M.: Chaotic attractors in incommensurate fractional order systems. Phys. D **237**, 2628-2637 (2008). http://dx.doi.org/10.1016/j.physd.2008.03.037
34. Li, F., Yao, C.: The infinite-scroll attractor and energy transition in chaotic circuit. Nonlinear Dynam. **84**, 2305–2315 (2016). doi:10.1007/s11071-016-2646-z
35. Sarasola, C., Torrealdea, F.J., d'Anjou, A., Moujahid, A., Graña, M.: Energy balance in feedback synchronization of chaotic systems. Phys. Rev. E **69**, 011606 (2004). https://doi.org/10.1103/PhysRevE.69.011606
36. Danca, M.-F., Kuznetsov, N., Chen, G.: Unusual dynamics and hidden attractors of the Rabinovich-Fabrikant system. Nonlinear Dynam., First online (2017). DOI: 10.1007/s11071-016-3276-1
37. Wu, X.J., Shen, S.L.: Chaos in the fractional-order Lorenz system. Int. J. Comput. Math. **86**, 1274-1282 (2009). http://dx.doi.org/10.1080/00207160701864426
38. Li, D., Lu, J., Wu, X., Chen, G.: Estimating the bounds for the Lorenz family of chaotic systems. Chaos Solitons Fract. 23, 529-534 (2005). http://dx.doi.org/10.1016/j.chaos.2004.05.021
39. Tavazoei, M., Haeri, M.: A proof for non existence of periodic solutions in time invariant fractional order systems. Automatica **45**, 1886-1890 (2009). http://dx.doi.org/10.1016/j.automatica.2009.04.001
40. Yazdani, M., Salarieh, H.: On the existence of periodic solutions in time-invariant fractional order systems. Automatica **47** 1834-1837 (2011). http://dx.doi.org/10.1016/j.automatica.2011.04.013

41. Kang, Y.-M., Xie, Y., Lu, J.C., Jiang, J.: On the nonexistence of non-constant exact periodic solutions in a class of the Caputo fractional-order dynamical systems. Nonlinear Dynam. **82**, 1259-1267 (2015). doi:10.1007/s11071-015-2232-9
42. Shen, J., Lam, J.: Non-existence of finite-time stable equilibria in fractional-order nonlinear systems. Automatica **50**, 547-551 (2014). http://dx.doi.org/10.1016/j.automatica.2013.11.018
43. Wang, J.R., Fečkan, M., Zhou, Y.: A survey on impulsive fractional differential equations. Fractional Calculus & Applied Analysis **19**, 806–831 (2016). https://doi.org/10.1515/fca-2016-0044
44. Dads, E.A., Benchohra, M., Hamani, S.: Impulsive fractional differential inclusions involving the Caputo fractional derivative. Fractional Calculus & Applied Analysis **12**, 15-38 (2009).
45. Gorenflo, R.: Fractional calculus: some numerical methods. In: Carpinteri A, Mainardi, F, editors. Fractals and Fractional Calculus in Continuum Mechanics; 1996. Vol. 378 of CISM Courses and Lectures p. 277-290, 1997.
46. Kilbas, A.A., Marzan, S.A.: Nonlinear differential equations with the Caputo fractional derivative in the space of continuously differentiable functions. Diff. Equat. **41** 84-89 (2005).
47. Li, C., Chen, Y.Q., Polubny, I., Vinagre, B.: Introduction to special issue: fractional dynamics and control. Int. J. Bifurcat. Chaos. Special Issue on Fractional Dynam. Control. 2012 (April).

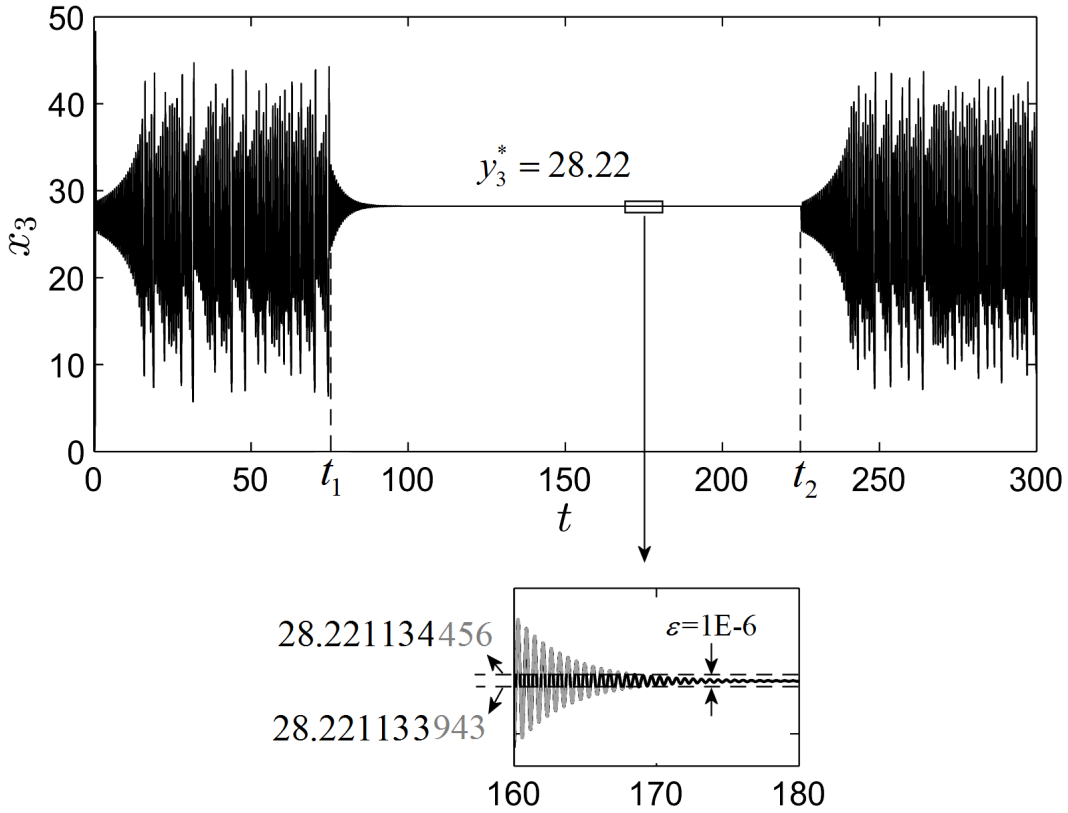

Fig. 1 Time series of the variable x_3 of the Lorenz system (6). For $t \in [t_1, t_2]$, the variable, denoted y_3^*, approximates the value 28.22. The zoomed rectangle reveals the approximation error determined in 6 decimals.

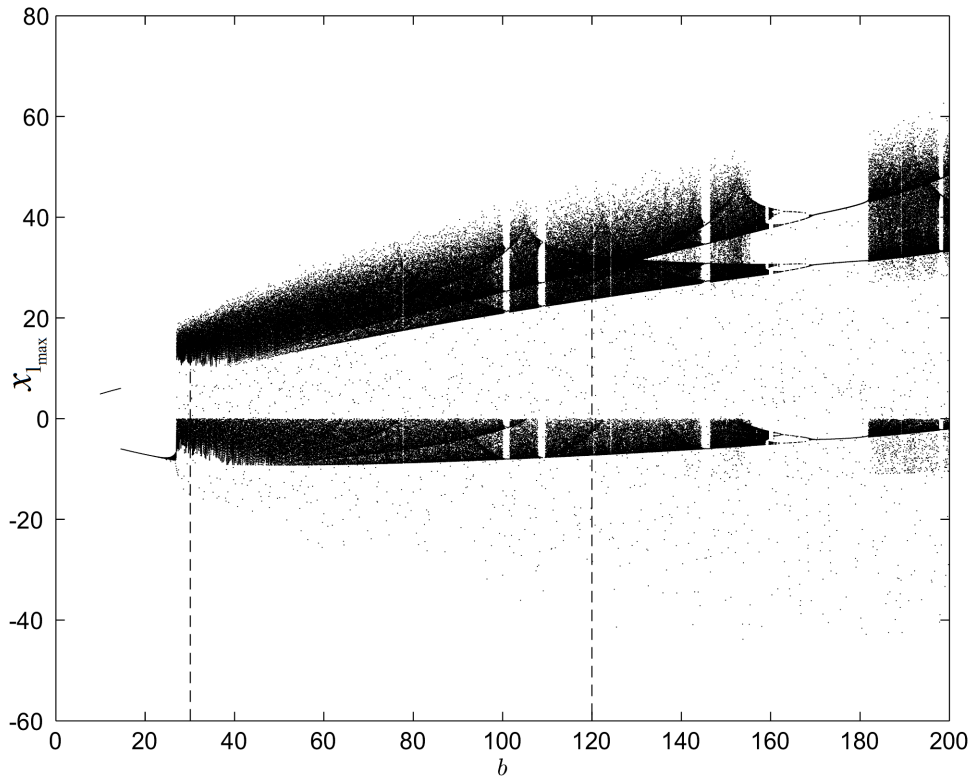

Fig. 2 Bifurcation diagram of the Lorenz system (6), with bifurcation parameter b .

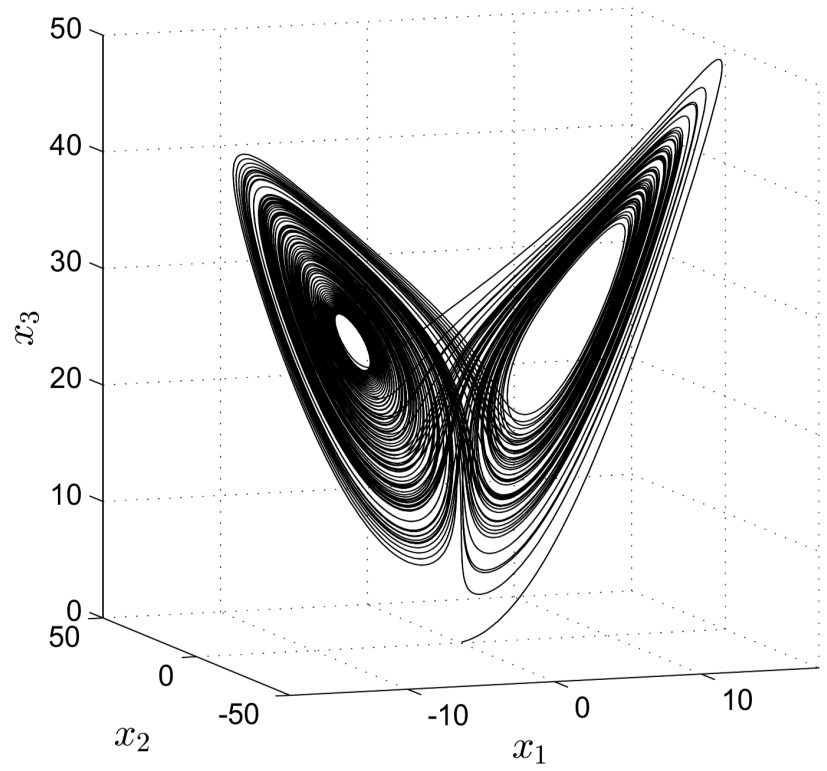

Fig. 3 Chaotic attractor of the fractional-order Lorenz system (6) with $b = 28$.

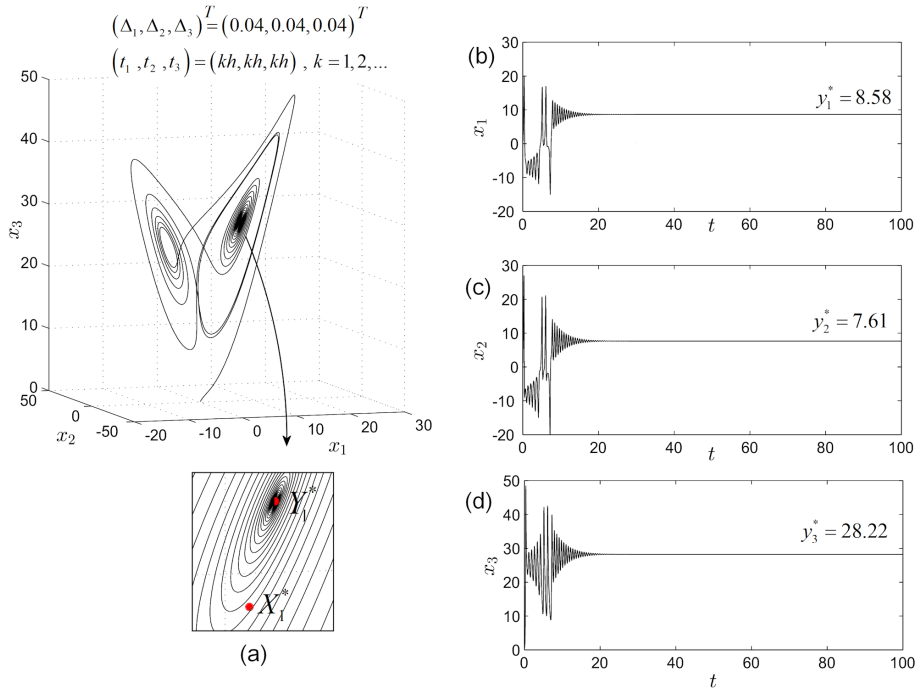

Fig. 4 Stable equilibrium Y_1^* obtained under control with impulses $(\Delta_1, \Delta_2, \Delta_3)^T = (0.04, 0.04, 0.04)^T$ applied at moments $(t_1, t_2, t_3) = (kh, kh, kh)$, $k = 1, 2, ..., N$. a) Phase portrait and zoomed detail revealing the distance between the unstable equilibria X_1^* and Y_1^*. b) Time series of x_1. c) Time series of x_2. d) Time series of x_3.

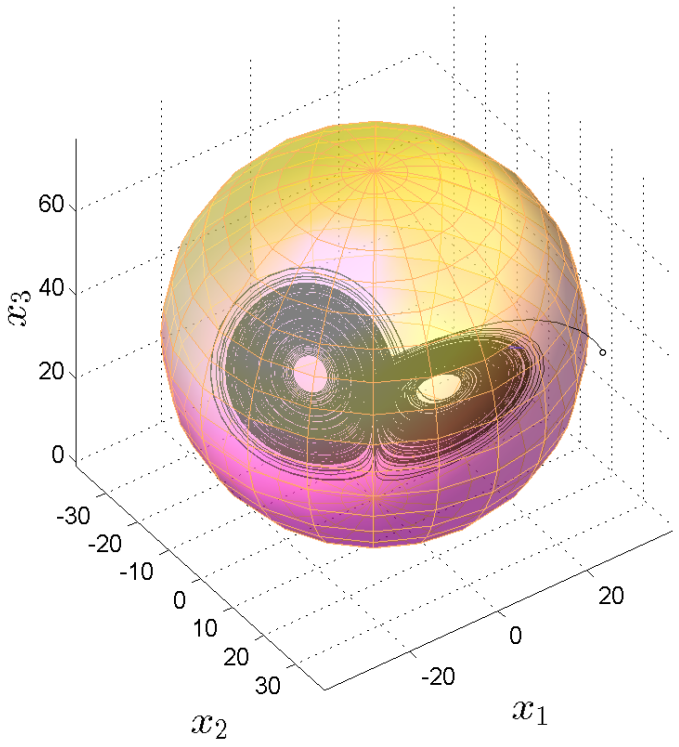

Fig. 5 The chaotic Lorenz attractor, with $b = 28$, included in the sphere $x_1^2 + x_2^2 + (x_3 - a - b)^2 \leq 39.25$.

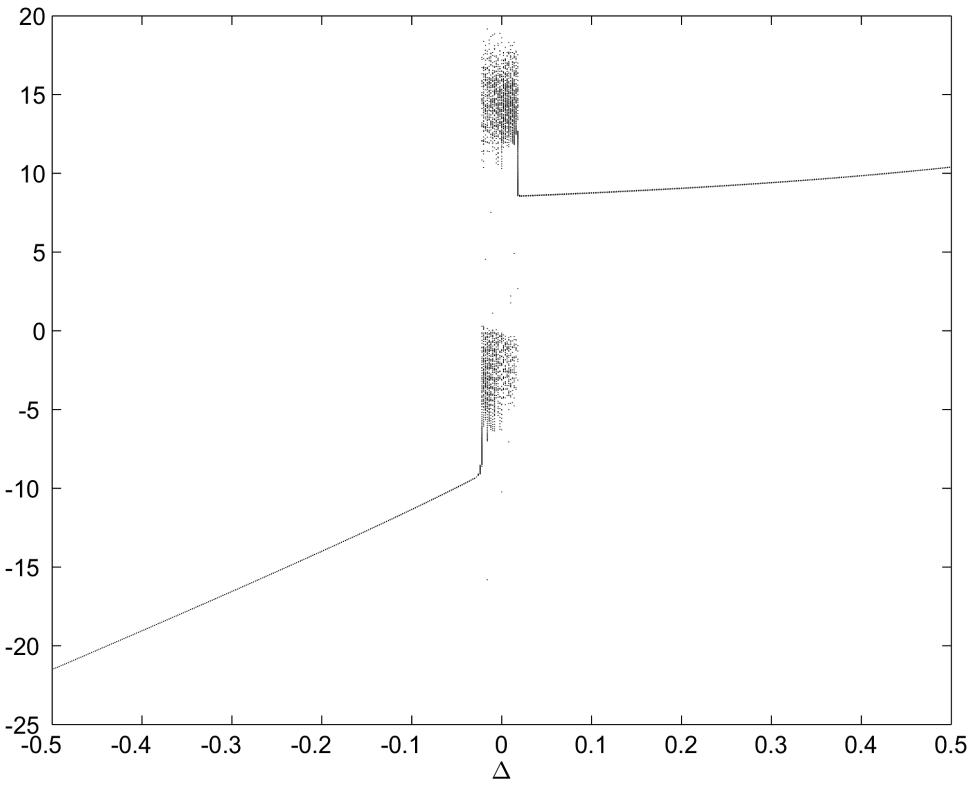

Fig. 6 Bifurcation diagram of the fractional-order Lorenz system (6) with $b = 28$ for $(\Delta_1, \Delta_2, \Delta_3)^T = (\Delta, \Delta, \Delta)^T$ bifurcation parameter.

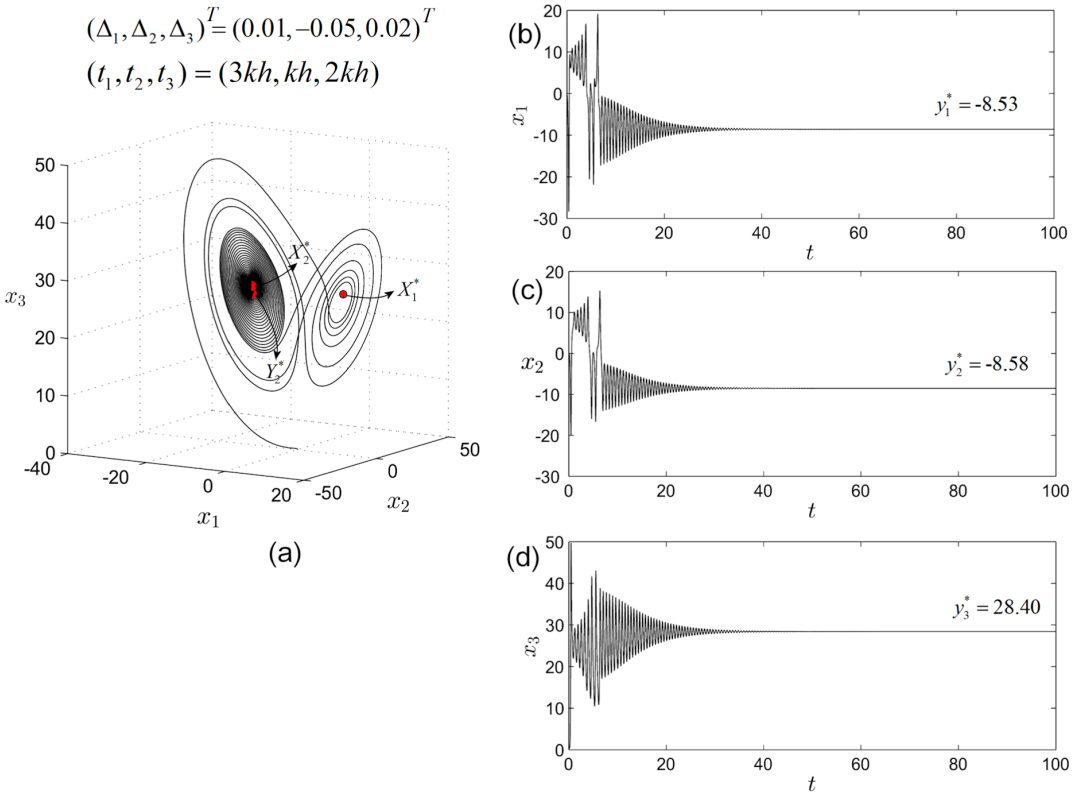

Fig. 7 Stable equilibrium Y_2^* obtained under control with impulses $(\Delta_1, \Delta_2, \Delta_3)^T = (0.01, -0.05, 0.02)^T$ applied at moments $t_1, t_2, t_3) = (3kh, kh, 2kh)$, $k = 1, 2, ..., N$. a) Phase portrait. b) Time series of x_1. c) Time series of x_2. d) Time series of x_3.

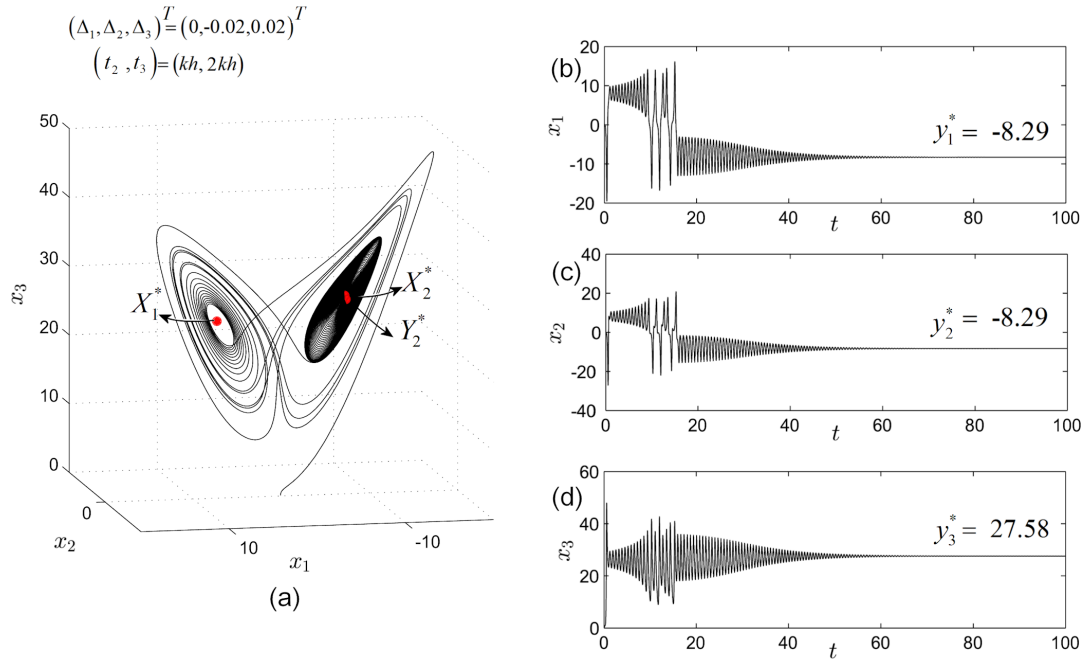

Fig. 8 Stable equilibrium Y_2^* obtained under control with impulses $(\Delta_1, \Delta_2, \Delta_3)^T = (0, -0.02, 0.02)^T$ applied at moments $(t_2, t_3) = (kh, 2kh)$. a) Phase portrait. b)-d) Time series.

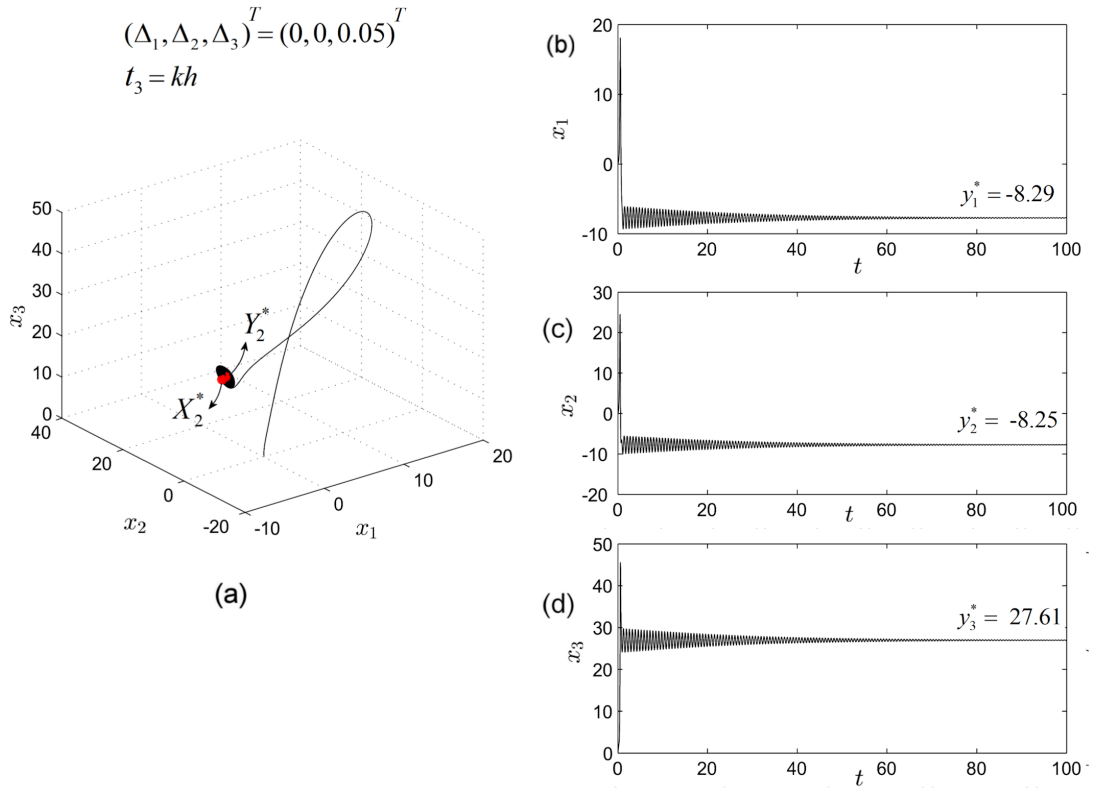

Fig. 9 Stable equilibrium Y_2^* obtained under control with impulses $(\Delta_1, \Delta_2, \Delta_3)^T = (0, -0.02, 0.02)^T$ applied at moments $(t_2, t_3) = (kh, kh)$ (only variables x_3 is impulsed). a) Phase portrait. b)-d) Time series.

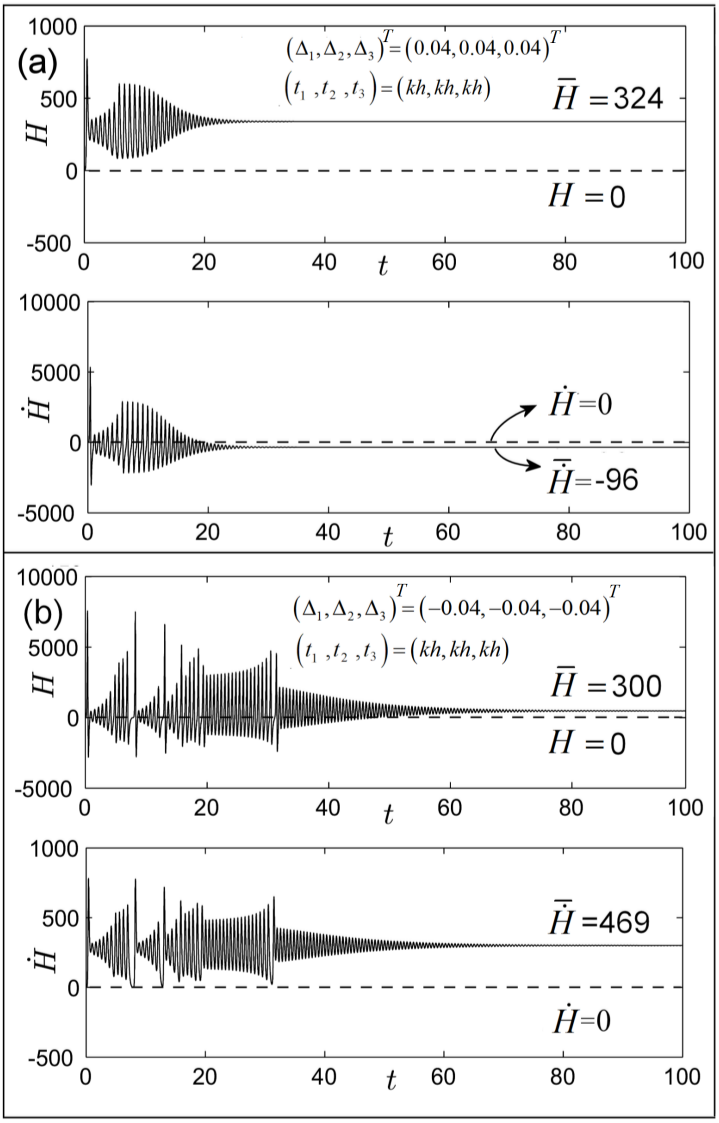

Fig. 10 Generalized energy H, its variation $\dot{H}$, and their averages. a) impulses $(\Delta_1, \Delta_2, \Delta_3)^T = (0, 04, 0.04, 0.04)^T$ applied at moments $(t_1, t_2, t_3) = (kh, kh, kh)$. b) impulses $(\Delta_1, \Delta_2, \Delta_3)^T = (-0, 04, -0.04, -0.04)^T$ applied at moments $(t_1, t_2, t_3) = (kh, kh, kh)$.

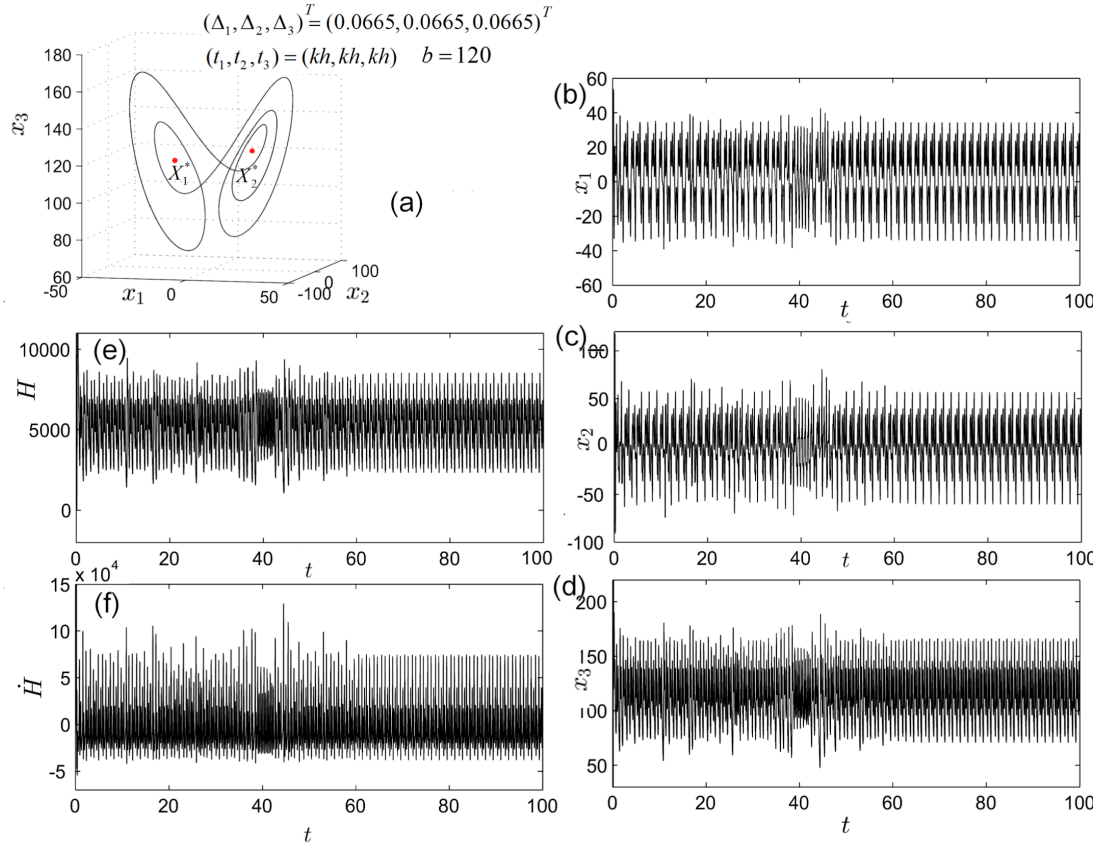

Fig. 11 Possible stable cycle, for $b = 120$, obtained under control with $(\Delta_1, \Delta_2, \Delta_3)^T = (0.0665, 0.0665, 0.0665)^T$ and $(t_1, t_2, t_3) = (kh, kh, kh)$. a) Phase plot. b)-d) Time series of the three components $x_{1,2,3}$. e) Generalized energy H. f) Derivation of the generalized energy $\dot{H}$.

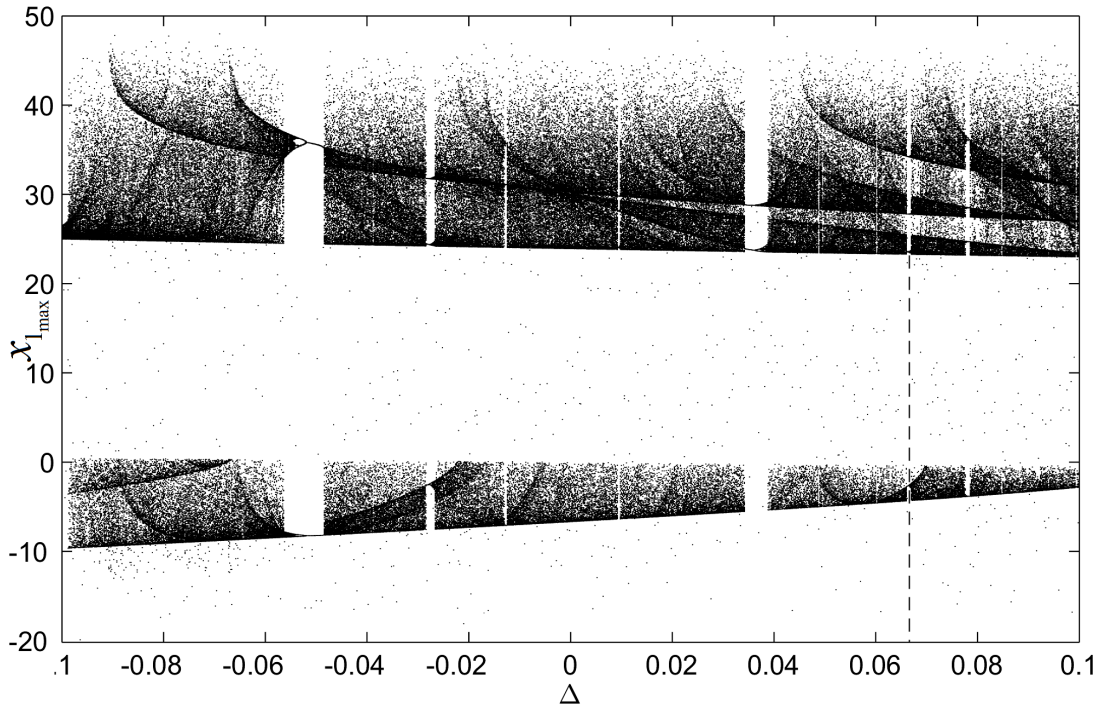

Fig. 12 Bifurcation diagram of the Lorenz system (6) with $b = 120$ for $(\Delta_1, \Delta_2, \Delta_3)^T = (\Delta, \Delta, \Delta)^T$ bifurcation parameter.